Clin Orthop Relat Res (2011) 469:2785–2795
DOI 10.1007/s11999-011-1856-4

SYMPOSIUM: CLINICALLY RELEVANT STRATEGIES FOR TREATING CARTILAGE AND MENISCAL PATHOLOGY

Integration of Tissue-engineered Cartilage With Host Cartilage: An In Vitro Model

John S. Theodoropoulos MD, J. N. Amritha De Croos PhD, Sam S. Park BSc, Robert Pilliar PhD, Rita A. Kandel MD

Published online: 15 March 2011

Abstract

Background We developed a tissue-engineered biphasic cartilage bone substitute construct which has been shown to integrate with host cartilage and differs from autologous osteochondral transfer in which integration with host cartilage does not occur.

Questions/purposes (1) Develop a reproducible in vitro model to study the mechanisms regulating tissue-engineered cartilage integration with host cartilage, (2) compare the integrative properties of tissue-engineered cartilage with autologous cartilage and (3) determine if chondrocytes from the in-vitro formed cartilage migrate across the integration site.

Methods A biphasic construct was placed into host bovine osteochondral explant and cultured for up to 8 weeks (n = 6 at each time point). Autologous osteochondral implants served as controls (n = 6 at each time point). Integration was evaluated histologically, ultrastructurally, biochemically and biomechanically. Chondrocytes used to form cartilage in vitro were labeled with carboxyfluorescein diacetate which allowed evaluation of cell migration into host cartilage.

Results Histologic assessment demonstrated that tissue-engineered cartilage integrated over time, unlike autologous osteochondral implant controls. Biochemically there was an increase in collagen content of the tissue-engineered implant over time but was well below that for native cartilage. Integration strength increased between 4 and 8 weeks as determined by a pushout test. Fluorescent cells were detected in the host cartilage up to 1.5 mm from the interface demonstrating chondrocyte migration.

Conclusions Tissue-engineered cartilage demonstrated improved integration over time in contrast to autologous osteochondral implants. Integration extent and strength increased with culture duration. There was chondrocyte migration from tissue-engineered cartilage to host cartilage.

Clinical Relevance This in vitro integration model will allow study of the mechanism(s) regulating cartilage integration. Understanding this process will facilitate enhancement of cartilage repair strategies for the treatment of chondral injuries.

One or more of the authors (RAK, RP) received funding from CIHR. This work was performed at CIHR-BioEngineering of Skeletal Tissues Team, Mount Sinai Hospital, Toronto, Canada.

J. S. Theodoropoulos (✉)
Orthopedic Surgery, Mount Sinai Hospital, 600 University Avenue, Suite 476C, Toronto M5G 1X5, Canada
e-mail: jtheodoropoulos@mtsinai.on.ca

J. N. A. De Croos, R. A. Kandel
Department of Pathology and Laboratory Medicine, CIHR-BioEngineering of Skeletal Tissues Team, Mount Sinai Hospital, Toronto, Canada

S. S. Park
Mount Sinai Hospital, 600 University Avenue, Suite 476C, Toronto M5G 1X5, Canada

R. Pilliar, R. A. Kandel
Institute of Biomaterials and Biomedical Engineering, University of Toronto, Toronto, Canada

Introduction

The goal of treating cartilage injuries is to restore joint congruency with hyaline cartilage and to integrate this neocartilage with surrounding host cartilage. Currently, there are a number of surgical options, including marrow-stimulating techniques such as microfracture [36], cartilage transplant techniques using either autograft or allograft

tissue [15, 16], and cell-based techniques such as autologous chondrocyte implantation (ACI) [7].

Microfracture techniques result in symptomatic improvement in young patients with improved functional and quality-of-life scores [4, 36]. Other studies have demonstrated lesions treated with microfracture can deteriorate after 2 years [26, 27], likely because of the high proportion of fibrocartilage that replaces the injured cartilage [26]. The need to find a cartilage replacement method resulting in hyaline cartilage repair led to the use of autologous osteochondral grafts. Unfortunately, these implants also deteriorate with time as a result of the lack of lateral integration between the host and donor cartilage [16, 24]. Other disadvantages include difficulty matching the donor plugs to the anatomy of the lesion and donor site morbidity [8]. To limit donor site morbidity, the use of fresh osteochondral allografts was popularized by Gross. His studies demonstrated long-term viability with 80% symptomatic relief at 10 years [15]. The histologic features associated with long-term survival of allografts include viability of chondrocytes and replacement of graft bone with host bone [15]. Nonetheless, lack of lateral integration was demonstrated in allograft implants harvested as long as 25 years after implantation [25]. Cell-based techniques such as ACI have shown superior repair cartilage with respect to both the amount of hyaline cartilage and integration with host cartilage [6, 16]. However, a study comparing microfracture with ACI demonstrated no difference in the amount of fibrocartilage and hyaline cartilage between the two treatment groups and none of the failures had a high hyaline cartilage content, suggesting the amount of hyaline cartilage present may influence subsequent failure [22].

Our group has developed a novel cartilage repair implant utilizing a biphasic construct that mimics an osteochondral implant and consists of cartilagenous tissue integrated to the intended articulation surface of a biodegradable porous bone substitute (calcium polyphosphate [CPP]) [20, 41]. There are several advantages to this approach. The in vitro formed cartilage tissue is already integrated with the underlying bone substitute and the CPP allows for bone ingrowth and fixation [32]. Furthermore, the cartilage tissue of this construct is hyaline-like, rich in Type II collagen and proteoglycans similar to native cartilage. In contrast to other repair methods, the implanted cartilage integrates with surrounding cartilage [39]. This suggests that this system could be used as a model to study factors influencing cartilage integration. As many cartilage repair methods fail because of poor integration, understanding factors that influence integration is critical.

Thus, the aims of this study were to: (1) Develop a reproducible in vitro model to study the mechanisms regulating tissue-engineered repair cartilage integration with native cartilage; (2) compare the integrative properties of the cartilage of tissue-engineered cartilage implant with an autologous osteochondral implant; and (3) determine if chondrocytes from the in vitro formed cartilage migrate across the integration site.

Materials and Methods

This study investigated the integration of tissue-engineered cartilage with host cartilage (experimental) and compared this to the integration of the cartilage of the autologous osteochondral implants with host cartilage (control). Each integration model (experimental and control) was analyzed histologically, biochemically, and biomechanically at 2 different culture time periods, 4 and 8 weeks ($n = 6$ at each time point). In addition, cell migration was evaluated in the experimental group at 4 and 8 weeks ($n = 6$ at each time point), to demonstrate if it occurs and whether the distance migrated increased with time.

To form tissue-engineered cartilage, full-thickness articular cartilage was harvested from bovine (6- to 9-month-old) metacarpal-phalangeal joints and chondrocytes isolated by sequential enzymatic digestion using 0.5% proteinase (Sigma-Aldrich Chemical Co, St Louis, MO) with 1% antibiotics (penicillin G, streptomycin sulphate, and amphotericin B; Invitrogen Co, Auckland, New Zealand) for 2 hours and 0.1% collagenase (Sigma-Aldrich Chemical Co) overnight under standard cell culture conditions as previously described [41]. The chondrocytes were then seeded at a density of 160,000 cells/mm^2 onto the top surface of 5.7-mm-diameter cylindrical discs of CPP surrounded by heat-shrinkable polyolefin tubing (3 M, Austin, TX). The tubing was prepared by placing the polyolefin over a 5.7-mm metal rod and autoclaved to yield a tube of the correct diameter. The tubing creates a well-like structure and prevents cell spillage from the surface of the CPP. The CPP substrates were manufactured as previously described [31].

The chondrocytes were grown in Ham's F12 supplemented with 5% fetal bovine serum (FBS). On Day 5, the serum concentration was increased to 20% FBS and ascorbic acid (100 μg/mL; Sigma-Aldrich Chemical Co) was added to the media. The constructs were grown for 7 days and were then placed into the integration model explant system.

To obtain the host osteochondral tissue, bovine calf metacarpal-phalangeal joints were exposed by an arthrotomy and using a mosaicplasty circular punch (4.5 mm; Smith and Nephew, Andover, MA), an osteochondral defect (4.5 mm × 10 mm) was created in the medial and lateral condyles (Fig. 1). This defect size ensured that the implant would fit tightly. A power drill with a 1.5-cm diamond-tipped circular drill bit was used to remove the osteochondral tissue surrounding the 4.5-mm defect from

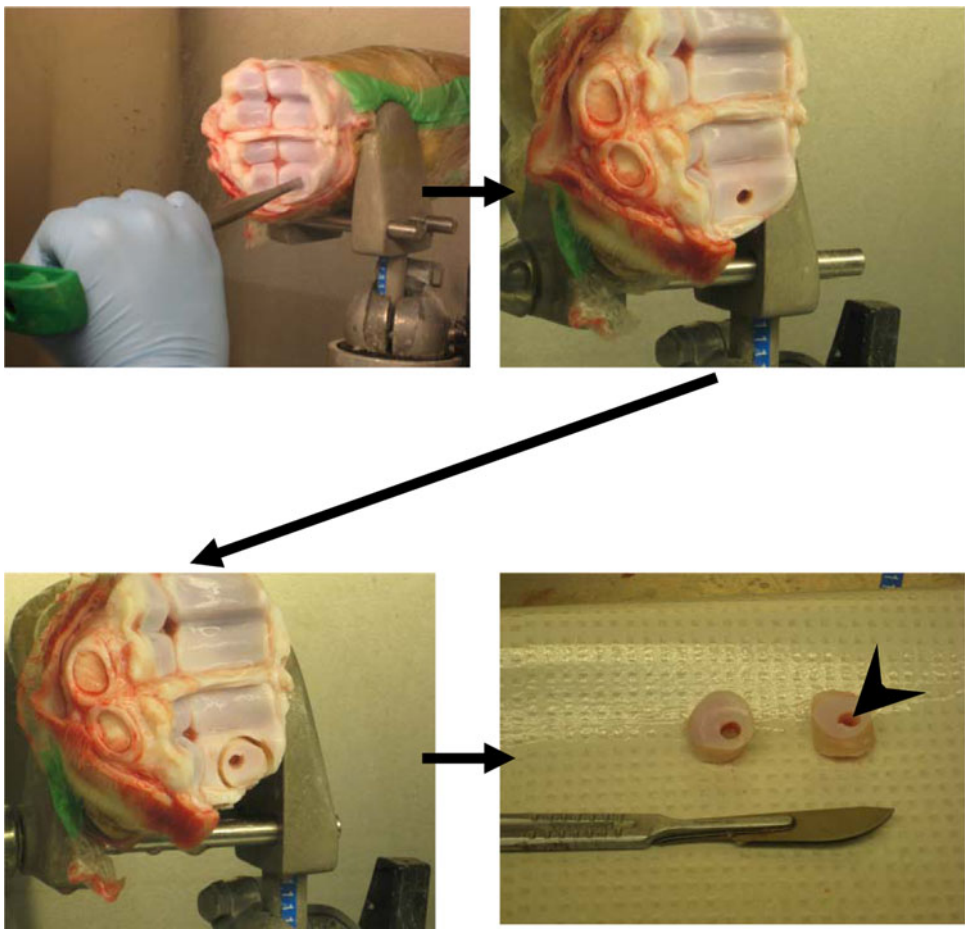

Fig. 1 The method utilized to form osteochondral host tissue explant. A doughnut-shaped osteochondral explant is generated from a segment of the bovine metacarpal-phalangeal joint. The arrowhead in the last panel points to the hole into which the implant will be placed.

the joint surface, thus creating a doughnut-shaped host osteochondral explant (rim of host cartilage surrounding the previously cored-out hole). The explants were then placed into 50-mL tubes (Becton Dickinson Labware Co, Franklin Lakes, NJ) containing phosphate-buffered saline (PBS) and subjected to three 20-minute washes in PBS. They were then transferred to 12-well plates (Becton Dickinson Labware Co) containing 3 mL of Ham's F12 media supplemented with 1% antibiotics and incubated overnight under standard tissue culture conditions. The next day, the in vitro-formed biphasic constructs were press-fit into the hole in the host osteochondral explant ($n = 6$ at each time point) (Fig. 2A). Autologous osteochondral implant controls (5.5-mm diameter) were generated in a similar fashion (Fig. 2B) ($n = 6$ for each time point). These implant-explant constructs were then placed in Ham's F-12 supplemented with 20% FBS and ascorbic acid (100 μg/mL) and the media was changed every 2 to 3 days. Samples were harvested at 4 or 8 weeks of culture and the cartilage removed from the underlying bone and/or CPP using a scalpel. Half of each sample was used for histology, the other half for biochemical analysis. For evaluation of the interface zone, representative tissue

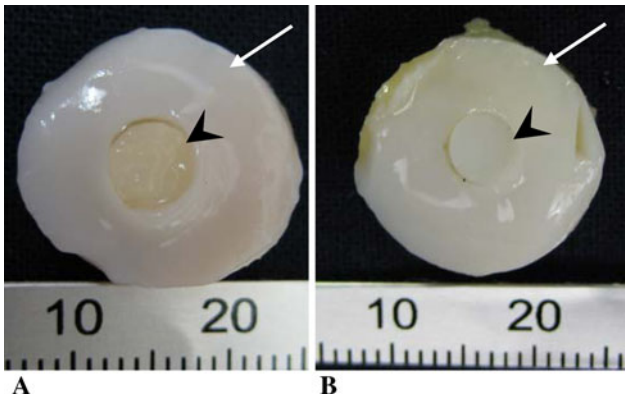

Fig. 2A–B The gross appearance of the constructs at the time of implantation. (**A**) The osteochondral host tissue (white arrow) implanted with either (**A**) a tissue-engineered cartilage implant (arrowhead) or (**B**) with the autologous osteochondral implant (arrowhead).

was taken, which included either tissue-engineered/host cartilage composite or the osteochondral implant control/host cartilage composite. The tissue was fixed in neutral-buffered 10% formalin (EMD Chemicals, Gibbstown, NJ)

and embedded in paraffin. Five-micron sections were cut, stained with either hematoxylin and eosin or toluidine blue, and examined by light microscopy. Representative samples of the interface were also fixed in 2% glutaraldehyde, infiltrated with Spurr resin (Electron Microscopy Sciences, Hatfield, PA), and examined by transmission electron microscopy (TEM) (TecNai 20; FEI, Eindhoven, The Netherlands).

The extent of integration was determined using light microscopy by calculating the percent of the total interface length between the implant and the surrounding host cartilage that was integrated (integration was defined as no gap between the tissues as visualized in a histologic section). The length of the complete integration surface between the implant and the surrounding host cartilage was measured. This was divided by the entire length of the interface between the implant and host cartilage and a percentage was determined. This was classified as 0% (no integration), 1% to 50%, 50% to 99%, or 100% (complete integration) and then each was assigned a value (0 = no integration, 1 = 1%–50%, 2 = 50%–99%, or 3 = 100%). The average integration score was determined for both the 4- and 8-week culture periods (n = 24 at 4 weeks and n = 21 at 8 weeks).

An 8-mm biopsy dermal punch was used to harvest host and implant cartilage for biochemical analysis. The in vitro and host tissues were separated from each other using a surgical blade and placed into separate tubes. Tissue was lyophilized overnight, the dry weight determined, and then digested with papain (Sigma-Aldrich Chemical Co; 40 μg/mL) for 48 hours at 65°C [41]. The digest was stored at −30°C until analysis.

DNA content was determined from aliquots of the papain digest using the Hoechst dye 33258 assay (Polysciences Inc, Warrington, PA) and fluorometry (excitation: 365 nm; emission: 458 nm). Calf thymus DNA was used to generate the standard curve [41]. The proteoglycan content was estimated by quantifying the amount of sulphated glycosaminoglycans using the dimethylmethylene blue dye binding assay (Polysciences Inc) and spectrophotometry (wavelength: 525 nm) [14]. The standard curve was generated using bovine trachea chondroitin sulfate (Sigma-Aldrich Chemical Co). Collagen content was estimated from the hydroxyproline content. Aliquots of the papain digest were hydrolyzed in 6 M HCl at 110°C for 18 hours and hydroxyproline content of the hydrozylate determined using chloramine-T/Ehrlich's reagent assay and spectrophotometry (wavelength: 560 nm) [19]. L-hydroxyproline (Sigma-Aldrich Chemical Co) was used to generate the standard curve.

To evaluate the strength of integration, the implant cartilage together with the adjacent host cartilage (diameter = 8 mm) was removed from the CPP and bone after 4 or 8 weeks (n = 6 at each time point). The tissue containing the integration site was placed on a custom-designed block and the outer host cartilage was fixed (Fig. 3) with Loctite Super-Glue (Henkel Corp, Avon, OH). Using an Instron 4301 mechanical testing apparatus (Norwood, MA), the implant tissue was loaded at a rate of 0.5 mm/min until the implant tissue was pushed out from the adjacent host tissue. The thickness of each sample was measured digitally at four quadrants and the average was used to calculate the interface area. Using LabView Data Acquisition software (Austin, TX), the peak shear stress was calculated by dividing the push out force by the interface area (4πT). During the pilot experiments, we found the autologous control constructs separated easily indicating a lack of integration and as a result, the pushout strength could not be determined for these samples.

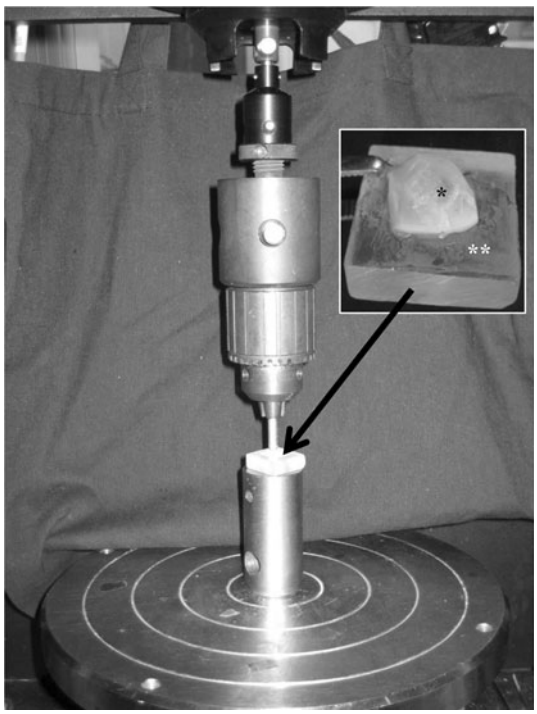

Fig. 3 An Instron 4301 mechanical testing apparatus applies a load to the central 4 mm of the tissue-engineered implant at a rate of 0.5 mm/min until the cartilage is pushed out. The inset shows tissue-engineered cartilage (*) and surrounding host tissue on a custom holding block (**).

To determine whether the cells in the tissue-engineered cartilage migrate into the adjacent surrounding host cartilage, in selected experiments, the chondrocytes were labeled with carboxyfluorescein diacetate (CFDA; Molecular Probes, Eugene, OR) according to the manufacturer's protocol. In previous studies, we demonstrated cell labeling had no effect on the ability of the cells to form tissue [2]. Briefly, chondrocytes isolated from bovine cartilage were incubated in suspension with CFDA (2.5 μM in PBS) for

15 minutes at 37°C. Cells were pelleted, washed twice in Ham's F-12 (30 minutes each), and then resuspended in Ham's F-12 supplemented with 5% FBS and seeded onto CPP discs as described previously. To evaluate the efficiency of labeling, an aliquot of cells were examined by fluorescent microscopy and > 95% of the cells were fluorescent. After either 4 or 8 weeks, the samples were harvested and the cartilage (tissue-engineered and adjacent host cartilage) removed from the bone and CPP with a scalpel. The tissue was fixed in 10% formalin and paraffin-embedded. Five-micron sections were cut, dewaxed, and then visualized unstained using a fluorescent microscope (Leica DMIL, Richmond Hill, ON, Canada; 492 nm excitation, 517 nm emission) connected to a computer and OpenLab software Version 3.1.4 (Leica DMIL). Images were captured at ×50 magnification and the light microscopic and fluorescent images were superimposed on each other using Adobe Photoshop CS software Version 8.0 (San Jose, CA) to create a composite image. The composite image was evaluated from the tissue-engineered implant cartilage, across the integration site, and into the host cartilage for a distance of 1.48 mm. Cell migration was quantified by counting both the number of labeled and unlabelled cells in the host cartilage contiguous after division of the host tissue into four quartiles (each measuring 0.37 mm). This also allowed us to quantify the distance the labeled cells had migrated into the host cartilage. The number of labeled cells in the four quartiles was then compared between the 4- and 8-week culture periods.

Our statistical analyses compared the mean response of various experimental variables in the tissue-engineered constructs and the autologous controls at both the 4- and 8-week culture periods. The response variables included the extent of integration, biochemical testing (DNA, hydroxyproline, and GAG content of the explant integration interface), and mechanical testing (maximum force to failure, normalized pushout force). For the extent of integration and cell migration responses, because no control group was available, a comparison of the mean response in the tissue-engineered constructs at 4 and 8 weeks was performed. These various two-sample comparisons were carried out using a two-sided Welch's t statistic [42]. To model the number of cells that migrated at the two time points (4 and 8 weeks) in the four different zones, we used a generalized linear model with a Poisson distribution for the cell count and a quasilikelihood estimation method to account for some overdispersion [1]. We also performed a one-sided Welch's t statistic to test a decrease in cell

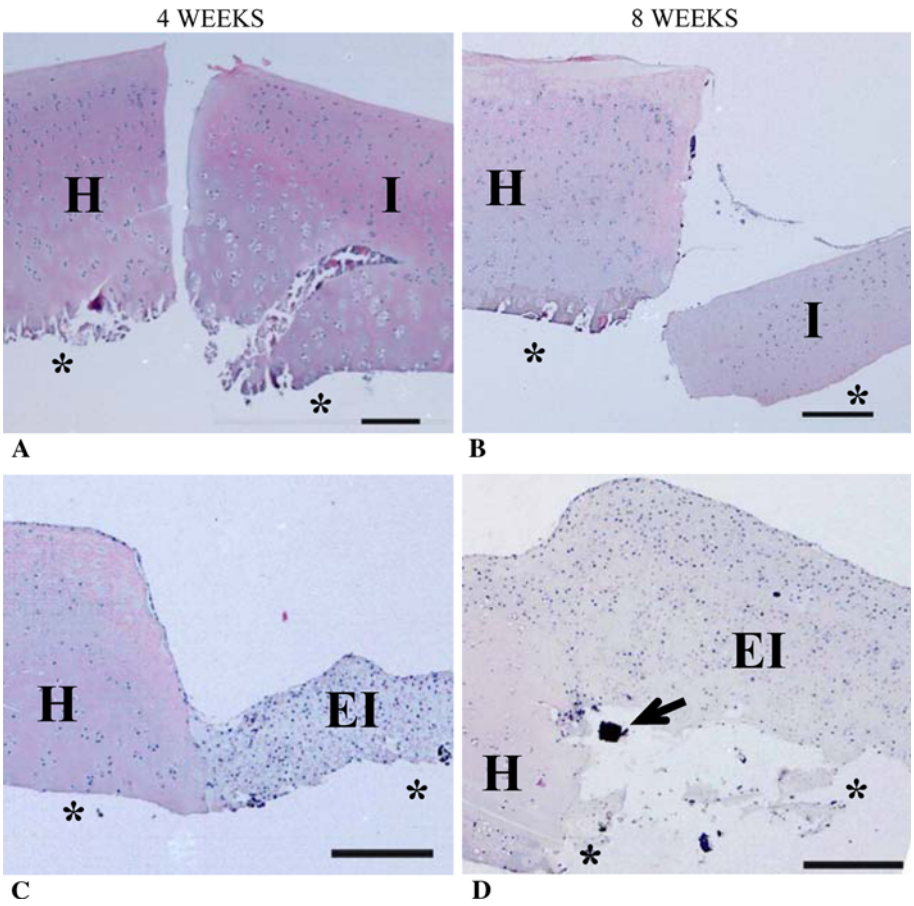

Fig. 4A–D These photomicrographs show the histologic appearance of implant tissue (**A**, **B**: osteochondral and **C**, **D**: tissue-engineered implant) and interfacing host tissue over time. *Indicates where bone and calcium polyphosphate (CPP) would be located if they had not been removed from the tissue. I = autologous implant tissue; EI = tissue-engineered implant tissue H = interfacing host tissue; ↑ = bone fragment. Scale bar = 0.25 mm (Stain, hematoxylin and eosin; original magnification, 50×).

counts at 8 weeks versus 4 weeks in each zone. The statistical software used was SPSS (Chicago, IL) and R (R Development Core Team, http://www.R-project.org).

Results

Macroscopic examination revealed the tissue-engineered host cartilage composites were integrated at both the 4- and 8-week culture periods. In contrast, the autologous osteochondral controls did not demonstrate any integration at either 4- and 8-week time points confirming integration did not improve with time.

Histologic assessment of the autologous control implants demonstrated that both the implant and surrounding cartilage were intact (Fig. 4A–B). However, no cells were seen in a narrow zone (up to 0.05 mm) adjacent to the integration site in most of the host cartilage explants suggesting chondrocyte death. There was no lateral integration at either 4 or 8 weeks as there was a continuous gap between the implanted cartilage and the surrounding host cartilage interface. In contrast, the tissue-engineered constructs demonstrated integration with the adjacent host cartilage (Fig. 4C–D), although the extent of integration was variable at 4 weeks (Fig. 5). TEM demonstrated thin collagen fibers similar to those seen in the tissue-engineered cartilage, at the interface region extending into the host cartilage (Fig. 6).

Tissue integration was semiquantified histologically. As autologous control implants did not show any integration histologically, no integration score could be determined for these samples. After 4 weeks, the percent integration of tissue-engineered implants with the surrounding host tissue was low (Fig. 5A). However, by 8 weeks, the distribution shifted toward a higher percent integration (Fig. 5A). The average score at 8 weeks (2.0 ± 0.2) was greater ($p = 0.002$) compared with 4 weeks (1.0 ± 0.2) (Fig. 5B; $n = 24$ at 4 weeks and $n = 21$ at 8 weeks).

Although histologically the tissue-engineered cartilage appeared more cellular than the surrounding host cartilage, there was no statistical difference in the DNA content normalized to dry weight at the 4- or 8-week time points between the tissue-engineered and autologous control cartilage (Fig. 7). As well, there were no differences in GAG content between the two at either time point. Hydroxyproline content was higher in the surrounding host cartilage compared with the tissue-engineered cartilage at both the 4- ($p = 0.009$) and 8- ($p = 0.003$) week intervals. As well, at 8 weeks, the hydroxyproline content was increased ($p = 0.009$) in the tissue-engineered implant compared with 4-week samples. The hydroxyproline content of the autologous cartilage control implant was similar to that in the host cartilage.

The tissue-engineered implants were tested using a pushout test to evaluate integration strength over time. The maximum force to failure of the 8-week samples (2.80 ± 0.6 N) compared with the 4-week samples (1.40 ± 0.3 N) was higher ($p = 0.002$, $n = 6$) (Fig. 8). The normalized pushout strength (maximum force normalized to integration area) for tissue-engineered constructs increased from the 4- to 8-week cultivation period from 56.7 ± 8.4 kPa to 120 ± 30.5 kPa.

CFDA-labeled fluorescent cells were seen in the host cartilage and were more numerous at 8 weeks as compared with 4 weeks. As well, the cells seemed to migrate further into the host tissue with time (Fig. 9). No difference ($p = 0.17$) in the number of labeled cells closest to the interface (Zone 1) at 8 weeks compared with 4 weeks was observed. However, by 8 weeks, there were more cells distant (beyond 0.37 mm) to the host cartilage edge in the three distal zones (Zone 2: $p = 0.05$: Zone 3: $p = 0.03$; and Zone 4: $p = 0.05$) (Table 1). No

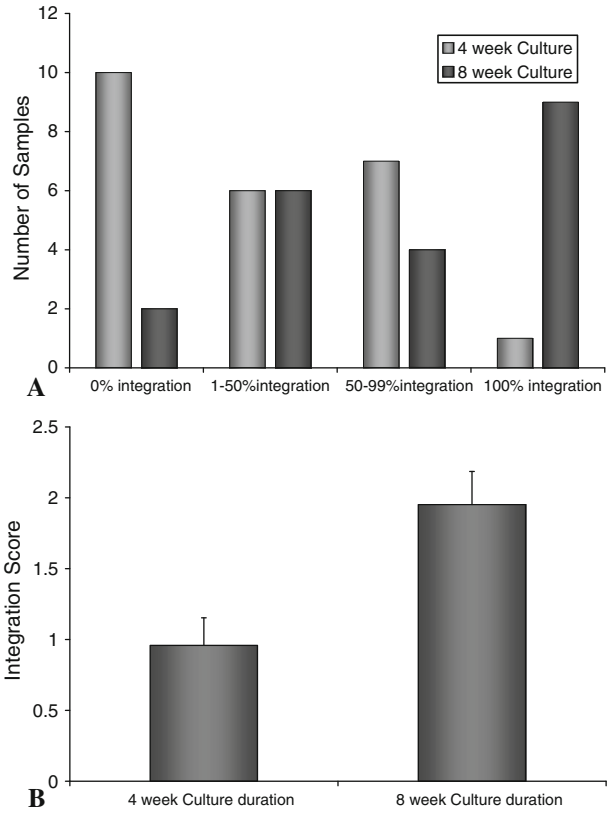

Fig. 5A–B The integration of tissue-engineered constructs with surrounding host tissue was evaluated semi-quantitatively. Light microscopy images were assessed for the extent of integration at 4 and 8 weeks. (**A**) Histogram showing the number of samples demonstrating the percent of integration. The distribution demonstrated a significant increase ($p = 0.002$) in integration with time when the average integration score at 4 and 8 weeks of culture were compared (**B**).

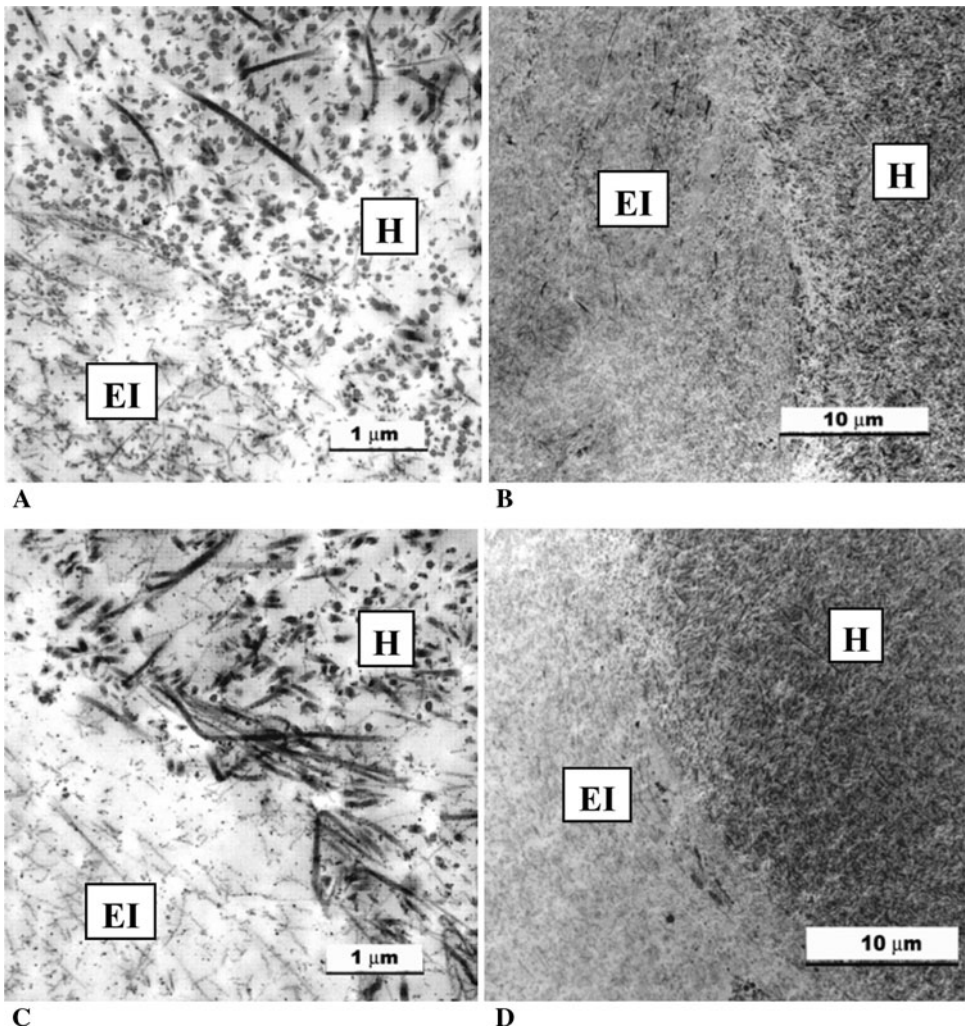

Fig. 6A–D Transmission electron microscopic images of the tissue-engineered implant and host cartilage interface at (**A**, **B**) 4 and (**C**, **D**) 8 weeks. The host cartilage was characterized by the presence of large collagen fibers, whereas the in vitro-formed cartilage had fewer collagen fibers that were smaller and thinner than those observed in the adjacent host tissue. At sites of integration, smaller fibers were seen admixed with the larger fibers. These interdigitating fibers were present by 4 weeks and seemed to increase in number with time. Both intact and necrotic chondrocytes were seen at the interface in some of the implants. EI = tissue-engineered implant tissue; H = interfacing host tissue.

fluorescent cells could be seen when unlabeled cells were used to form the cartilage confirming chondrocytes were not autofluorescent.

Discussion

Integration with the surrounding cartilage is critical for successful cartilage repair to provide normal stress distribution with weightbearing and prevent future tissue degeneration [12]. We compared cartilage integration of tissue-engineered biphasic constructs to autologous osteochondral implants histologically, ultrastructurally, biomechanically, and biochemically. In addition, chondrocyte migration from tissue-engineered cartilage to host cartilage was evaluated.

Our study has a number of limitations. First, this is an in vitro system so it is not subjected to the in vivo environment such as the presence of inflammatory cells or synovial fluid, conditions that can affect chondrocyte function. Second, it is a static model and is not subjected to weightbearing, which may also influence integration. However, in spite of these two limitations the model clearly mimics what happens in vivo, that is, lateral integration of tissue-engineered cartilage to host cartilage. Third, some chondrocytes demonstrated loss of fluorescence with time in culture while others continued to demonstrate strong fluorescence. This loss of fluorescence may have occurred as a result of cell division. However, this was not considered significant as our goal was not to define an absolute number of cells that migrated across the integration zone but to demonstrate that cell migration does occur. Finally, the integration strength of the tissue-engineered construct did not reach the levels of native cartilage. However, we presume this is not critical to the model as it does show increasing strength over time. It is possible the integration strength may reach that of native cartilage with longer culture periods and this will be investigated in future studies.

Using in vitro-formed and native osteochondral plugs, we demonstrated this model system recapitulates what

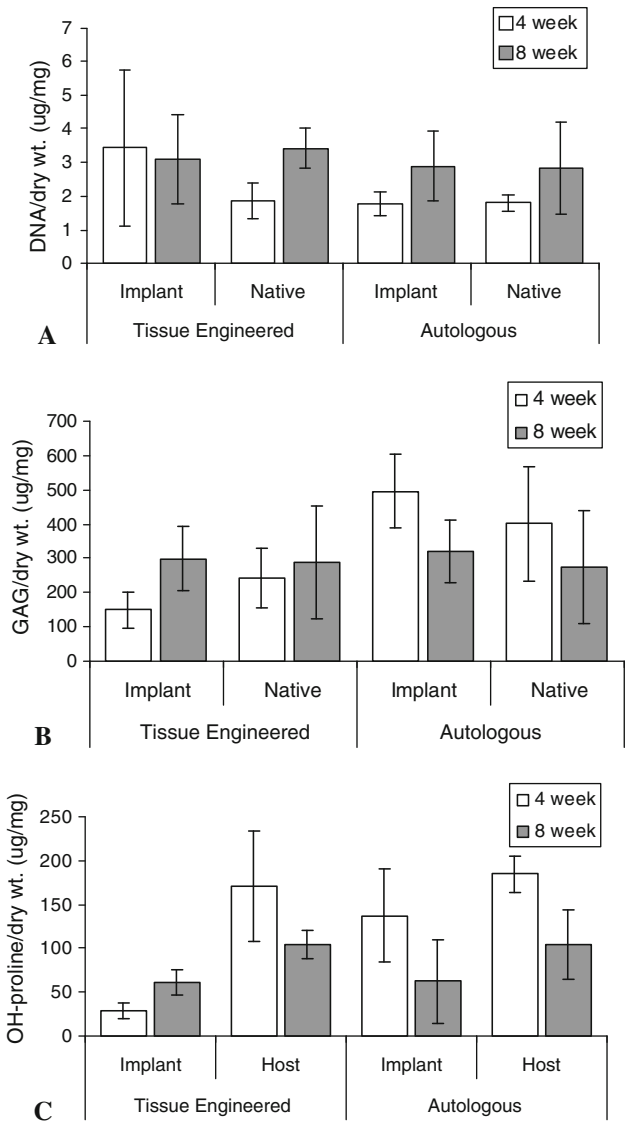

Fig. 7A–C At 4 weeks (white bars) and 8 weeks (gray bars) of culture, the implant and host tissues were assessed for (**A**) DNA, (**B**) GAG, and (**C**) OH-proline content. These were normalized to dry weight and expressed as mean ± SEM.

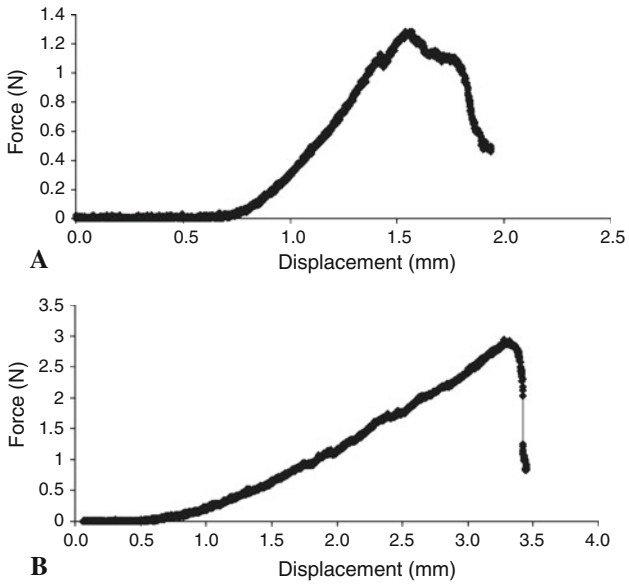

Fig. 8A–B Representative stress-strain curves for (**A**) 4- and (**B**) 8-week-old samples used to determine the pushout strength of the integration of the tissue-engineered implant and host cartilage are shown.

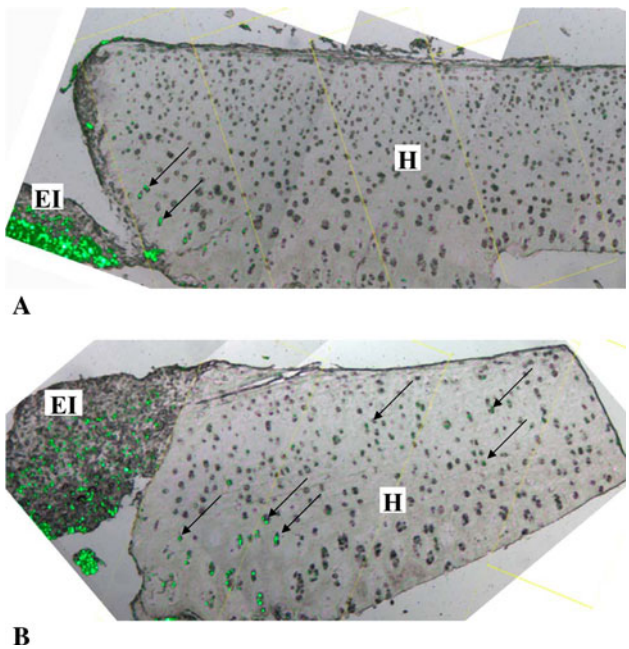

Fig. 9A–B Unstained light microscopic and fluorescent images of tissues at (**A**) 4 and (**B**) 8 weeks of culture were captured at ×50 magnification and superimposed on each other using Adobe Photoshop CS software Version 8.0 to create a composite image of each sample. Arrows point to carboxyfluorescein diacetate (CFDA)-positive cells (green) that have migrated into the host cartilage. EI = tissue-engineered implant tissue; H = host tissue.

occurs in vivo, eg, integration of tissue-engineered cartilage with host cartilage and no integration of the cartilage of autologous osteochondral implants. Furthermore, the extent and strength of integration were both shown to increase with time. Importantly, the DNA content of these tissues under these conditions did not change between 4 and 8 weeks. Interestingly, integration occurred although the adjacent host cartilage had a hypocellular zone, a feature others have shown prevents (or limits) integration [29, 30, 34]. This finding suggests repair cartilage may be primarily responsible for integration. Although we do not yet know the mechanism(s) regulating integration, our findings suggest the process may involve collagen production and cell migration. The contribution of collagen to integration was demonstrated by ultrastructural examination of the integration site. This revealed collagen fibers similar to those seen in repair cartilage in the native

Table 1. Evaluation of chondrocyte migration across the integration zone*

Culture time	Conditions	Zone 1 0–0.37 mm	Zone 2 0.37–0.74 mm	Zone 3 0.74–1.1 mm	Zone 4 1.1–1.5 mm
4 weeks	Total number of cells counted	86.8 ± 35.9	124.8 ± 43.6	134.7 ± 45.0	106 ± 36.4
	Percent CFDA-labeled cells	35.9 ± 14.9	13.8 ± 5.0	12.1 ± 7.4	15.8 ± 12.3
8 weeks	Total number of cells counted	72.0 ± 24.4	97.8 ± 38.3	92.0 ± 43.2	66.7 ± 39.9
	Percent CFDA-labeled cells	55.1 ± 22.6	30.7 ± 18.8	34.3 ± 16.5	40.7 ± 23.3

* Chondrocytes were labeled with CFDA and the number of fluorescent CFDA-labeled chondrocytes present in the native cartilage and the distance migrated into the host cartilage over time was quantified as described under the Materials and Methods; Zone 1 is adjacent to the interface and Zone 4 is the farthest from the interface; CFDA = carboxyfluorescein diacetate.

cartilage, at the integration site, only where there was a continuous interface between the tissue-engineered cartilage and the surrounding host tissue. Biochemical analysis also supported a role for collagen as there was an increase in collagen content in the tissue-engineered implants between 4 and 8 weeks. In contrast, there was no difference in cellularity or proteoglycan content between the tissue-engineered cartilage and the cartilage of the osteochondral plug. Ahsan et al. reported that collagen deposition contributed to cartilage integration in their in vitro model system, as inhibition of collagen crosslinking inhibited integration [3]. In another study integration between live and devitalized cartilage has been shown to be dependent on collagen deposition [12].

Ideally, the biomechanical properties of the integration site should be near that of native tissue. Our study measured the strength of the interface of tissue-engineered cartilage/host cartilage, which was not held together with fibrin glue or sutures, as has been used in some other investigations [29, 35]. Although the strength of integration increased over time by 8 weeks it was still an order of magnitude less than the pushout strength of intact healthy cartilage (8.8 MPa) [40]. However, it was almost fivefold higher (28 kPa at 4 weeks) than that observed in another in vitro model [38]. It may be that with even longer culture periods or mechanical loading that the strength of integration will continue to improve. The absence of substantial integration of the native osteochondral implants in our model mimics what occurs in vivo in mosaicplasty confirming the appropriateness of our model.

It has been speculated that the inability of chondrocytes to migrate to a site of injury may be the reason for inferior repair of damaged cartilage [21]. Our study showed that bovine chondrocytes are motile although their role in cartilage repair and integration in this model is unknown. Previous studies in our laboratory have highlighted the importance of matrix remodeling, mediated in part by the protease MT1-MMP, in improving tissue formation [9, 10]. Given the role of MT1-MMP in cell migration [11, 37], it is possible this metalloprotease is involved in chondrocyte motility; however, further study is required to confirm this.

Although there was cell death on the host side in our model, the engineered tissue was still able to integrate. This is contrary to other studies showing inhibition of cell death was essential in promoting integration [13, 21]. We do not know why our system differs in this respect, but it may be that the extent of contact between the implant and surrounding tissue is critical for the efficacy of integration. As a result of the surgical technique, a tight press-fit was achieved, a feature shown by others to improve stability and subsequent integration [23]. Huang et al. has demonstrated cartilage incongruity is not as well tolerated in osteochondral grafting in fracture management [17]. Furthermore, we observed samples that were countersunk or left proud did not integrate well (data not shown), supporting the importance of surgical technique and matching cartilage height to facilitate integration. It is possible that a close fit facilitates cell migration.

Spindle cell overgrowth (pannus-like tissue) onto the surrounding cartilage was also observed in some samples at both the 4- and 8-week time points. Interestingly, this did not appear to change over time. Others studies examining cartilage integration have also observed fibrous tissue overgrowth [28, 33] and that removing the tissue overgrowth resulted in decreased biomechanical pushout strength suggesting its presence may lead to an overestimation of integrative strength [28].

Many factors have been shown to undermine the integration of repair cartilage with native cartilage. Articular cartilage does not have a vascular supply and nutrients must come from synovial fluid making spontaneous repair difficult [5]. Current surgical techniques have been shown to cause cell death at the cut surfaces. The low cellularity of surrounding cartilage may not be able to compensate for this chondrocyte loss [18]. Thus, the advantage tissue-engineered cartilage implants may have over current autologous transplants is the high cellularity and, as shown here, the potential for some cells to migrate across the integration zone. Understanding the mechanisms regulating

the integrative process is important because we know that in the long term, if integration does not occur, then cartilage replacement strategies will go on to deteriorate and fail [18].

Acknowledgments We acknowledge Mr. H. Bojarski and Ryding-Regency Meat Packers for providing tissue samples and Dr Eugene Hu in the manufacture of the CPP substrates. As well, we thank Dr Jian Wang for help with the mechanical testing of the implants and Dr Laurent Briollais for help in the statistical analysis.

References

1. Agresti A. *Categorical Data Analysis.* New York: Wiley-Interscience; 2002.
2. Ahmed N, Gan L, Nagy A, Zheng J, Wang C, Kandel RA. Cartilage tissue formation using redifferentiated passaged chondrocytes in vitro. *Tissue Eng Part A.* 2009;15:665–673.
3. Ahsan T, Lottman LM, Harwood F, Amiel D, Sah RL. Integrative cartilage repair: inhibition by beta-aminopropionitrile. *J Orthop Res.* 1999;17:850–857.
4. Asik M, Ciftci F, Sen C, Erdil M, Atalar A. The microfracture technique for the treatment of full-thickness articular cartilage lesions of the knee: midterm results. *Arthroscopy.* 2008;24:1214–1220.
5. Athanasiou KA, Shah AR, Hernandez RJ, LeBaron RG. Basic science of articular cartilage repair. *Clin Sports Med.* 2001;20:223–247.
6. Briggs TW, Mahroof S, David LA, Flannelly J, Pringle J, Bayliss M. Histological evaluation of chondral defects after autologous chondrocyte implantation of the knee. *J Bone Joint Surg Br.* 2003;85:1077–1083.
7. Brittberg M, Tallheden T, Sjogren-Jansson B, Lindahl A, Peterson L. Autologous chondrocytes used for articular cartilage repair: an update. *Clin Orthop Relat Res.* 2001;391(Suppl):S337–348.
8. Browne JE, Branch TP. Surgical alternatives for treatment of articular cartilage lesions. *J Am Acad Orthop Surg.* 2000;8:180–189.
9. De Croos JN, Jang B, Dhaliwal SS, Grynpas MD, Pilliar RM, Kandel RA. Membrane type-1 matrix metalloproteinase is induced following cyclic compression of in vitro grown bovine chondrocytes. *Osteoarthritis Cartilage.* 2007;15:1301–1310.
10. De Croos JN, Roughley PJ, Kandel RA. Improved bioengineered cartilage tissue formation following cyclic compression is dependent on upregulation of MT1-MMP. *J Orthop Res.* 2010;28:921–927.
11. Deryugina EI, Bourdon MA, Reisfeld RA, Strongin A. Remodeling of collagen matrix by human tumor cells requires activation and cell surface association of matrix metalloproteinase-2. *Cancer Res.* 1998;58:3743–3750.
12. DiMicco MA, Sah RL. Integrative cartilage repair: adhesive strength is correlated with collagen deposition. *J Orthop Res.* 2001;19:1105–1112.
13. Gilbert SJ, Singhrao SK, Khan IM, Gonzalez LG, Thomson BM, Burdon D, Duance VC, Archer CW. Enhanced tissue integration during cartilage repair in vitro can be achieved by inhibiting chondrocyte death at the wound edge. *Tissue Eng Part A.* 2009;15:1739–1749.
14. Goldberg RL, Kolibas LM. An improved method for determining proteoglycans synthesized by chondrocytes in culture. *Connect Tissue Res.* 1990;24:265–275.
15. Gross AE, Kim W, Las Heras F, Backstein D, Safir O, Pritzker KP. Fresh osteochondral allografts for posttraumatic knee defects: long-term followup. *Clin Orthop Relat Res.* 2008;466:1863–1870.
16. Horas U, Pelinkovic D, Herr G, Aigner T, Schnettler R. Autologous chondrocyte implantation and osteochondral cylinder transplantation in cartilage repair of the knee joint. A prospective, comparative trial. *J Bone Joint Surg Am.* 2003;85:185–192.
17. Huang FS, Simonian PT, Norman AG, Clark JM. Effects of small incongruities in a sheep model of osteochondral autografting. *Am J Sports Med.* 2004;32:1842–1848.
18. Hunziker EB. Articular cartilage repair: basic science and clinical progress. A review of the current status and prospects. *Osteoarthritis Cartilage.* 2002;10:432–463.
19. Woessner JF. Determination of hydroxyproline content in connective tissues. In: Hall DA, ed. *The Methodology of Connective Tissue Research.* Oxford: Joynson-Bruvvers Limited; 1976.
20. Kandel RA, Grynpas M, Pilliar R, Lee J, Wang J, Waldman S, Zalzal P, Hurtig M. Repair of osteochondral defects with biphasic cartilage-calcium polyphosphate constructs in a sheep model. *Biomaterials.* 2006;27:4120–4131.
21. Khan IM, Gilbert SJ, Singhrao SK, Duance VC, Archer CW. Cartilage integration: evaluation of the reasons for failure of integration during cartilage repair. A review. *Eur Cell Mater.* 2008;16:26–39.
22. Knutsen G, Drogset JO, Engebretsen L, Grontvedt T, Isaksen V, Ludvigsen TC, Roberts S, Solheim E, Strand T, Johansen O. A randomized trial comparing autologous chondrocyte implantation with microfracture. Findings at five years. *J Bone Joint Surg Am.* 2007;89:2105–2112.
23. Kordas G, Szabo JS, Hangody L. Primary stability of osteochondral grafts used in mosaicplasty. *Arthroscopy.* 2006;22:414–421.
24. Lane JG, Massie JB, Ball ST, Amiel ME, Chen AC, Bae WC, Sah RL, Amiel D. Follow-up of osteochondral plug transfers in a goat model: a 6-month study. *Am J Sports Med.* 2004;32:1440–1450.
25. Maury AC, Safir O, Heras FL, Pritzker KP, Gross AE. Twenty-five-year chondrocyte viability in fresh osteochondral allograft. A case report. *J Bone Joint Surg Am.* 2007;89:159–165.
26. Mithoefer K, McAdams T, Williams RJ, Kreuz PC, Mandelbaum BR. Clinical efficacy of the microfracture technique for articular cartilage repair in the knee: an evidence-based systematic analysis. *Am J Sports Med.* 2009;37:2053–2063.
27. Mithoefer K, Williams RJ 3rd, Warren RF, Potter HG, Spock CR, Jones EC, Wickiewicz TL, Marx RG. The microfracture technique for the treatment of articular cartilage lesions in the knee. A prospective cohort study. *J Bone Joint Surg Am.* 2005;87:1911–1920.
28. Moretti M, Wendt D, Schaefer D, Jakob M, Hunziker EB, Heberer M, Martin I. Structural characterization and reliable biomechanical assessment of integrative cartilage repair. *J Biomech.* 2005;38:1846–1854.
29. Obradovic B, Martin I, Padera RF, Treppo S, Freed LE, Vunjak-Novakovic G. Integration of engineered cartilage. *J Orthop Res.* 2001;19:1089–1097.
30. Petersen JP, Ueblacker P, Goepfert C, Adamietz P, Baumbach K, Stork A, Rueger JM, Poertner R, Amling M, Meenen NM. Long term results after implantation of tissue engineered cartilage for the treatment of osteochondral lesions in a minipig model. *J Mater Sci Mater Med.* 2008;19:2029–2038.
31. Pilliar RM, Filiaggi MJ, Wells JD, Grynpas MD, Kandel RA. Porous calcium polyphosphate scaffolds for bone substitute applications—in vitro characterization. *Biomaterials.* 2001;22:963–972.
32. Pilliar RM, Kandel RA, Grynpas MD, Zalzal P, Hurtig M. Osteochondral defect repair using a novel tissue engineering

approach: sheep model study. *Technol Health Care.* 2007;15: 47–56.
33. Reindel ES, Ayroso AM, Chen AC, Chun DM, Schinagl RM, Sah RL. Integrative repair of articular cartilage in vitro: adhesive strength of the interface region. *J Orthop Res.* 1995;13:751–760.
34. Shapiro F, Koide S, Glimcher MJ. Cell origin and differentiation in the repair of full-thickness defects of articular cartilage. *J Bone Joint Surg Am.* 1993;75:532–553.
35. Silverman RP, Bonasser L, Passaretti D, Randolph MA, Yaremchuk MJ. Adhesion of tissue-engineered cartilate to native cartilage. *Plast Reconstr Surg.* 2000;105:1393–1398.
36. Steadman JR, Briggs KK, Rodrigo JJ, Kocher MS, Gill TJ, Rodkey WG. Outcomes of microfracture for traumatic chondral defects of the knee: average 11-year follow-up. *Arthroscopy.* 2003;19:477–484.
37. Takino T, Watanabe Y, Matsui M, Miyamori H, Kudo T, Seiki M, Sato H. Membrane-type 1 matrix metalloproteinase modulates focal adhesion stability and cell migration. *Exp Cell Res.* 2006; 312:1381–1389.
38. Tam HK, Srivastava A, Colwell CW, Jr., D'Lima DD. In vitro model of full-thickness cartilage defect healing. *J Orthop Res.* 2007;25:1136–1144.
39. Tognana E, Chen F, Padera RF, Leddy HA, Christensen SE, Guilak F, Vunjak-Novakovic G, Freed LE. Adjacent tissues (cartilage, bone) affect the functional integration of engineered calf cartilage in vitro. *Osteoarthritis Cartilage.* 2005;13:129–138.
40. van de Breevaart Bravenboer J, In der Maur CD, Bos PK, Feenstra L, Verhaar JA, Weinans H, van Osch GJ. Improved cartilage integration and interfacial strength after enzymatic treatment in a cartilage transplantation model. *Arthritis Res Ther.* 2004;6:R469–476.
41. Waldman SD, Grynpas MD, Pilliar RM, Kandel RA. Characterization of cartilagenous tissue formed on calcium polyphosphate substrates in vitro. *J Biomed Mater Res.* 2002;62:323–330.
42. Welch BL. The generalisation of student's problems when several different population variances are involved. *Biometrika.* 1947;34:28–35.